REAL-TIME PHYSICAL MODEL FOR ANALOG TAPE MACHINES

Jatin Chowdhury

Center for Computer Research in Music and Acoustics
Stanford University
Palo Alto, CA
jatin@ccrma.stanford.edu

ABSTRACT

For decades, analog magnetic tape recording was the most popular method for recording music, but has been replaced over the past 30 years first by DAT tape, then by DAWs and audio interfaces [1]. Despite being replaced by higher quality technology, many have sought to recreate a "tape" sound through digital effects, despite the distortion, tape "hiss", and other oddities analog tape produced. The following paper describes the general process of creating a physical model of an analog tape machine starting from basic physical principles, then discusses in-depth a real-time implementation of a physical model of a Sony TC-260 tape machine.

"Whatever you now find weird, ugly, uncomfortable, and nasty about a new medium will surely become its signature. CD distortion, the jitteriness of digital video, the crap sound of 8-bit - all of these will be cherished and emulated as soon as they can be avoided." -Brian Eno [2].

1. CONTINUOUS TIME SYSTEM

Audio recorded to and played back from a tape machine can be thought of as going through three distinct processors: the record head, tape magnetisation, and the play head.

1.1. The Record Head

For an instantaneous input current $I(t)$, the magnetic field output of the record head is given as a function of distance along the tape (x), and depth into the tape (y). Using the Karlqvist medium field approximation, we find [3]:

$$H_x(x,y) = \frac{1}{\pi} H_0 \Big(\tan^{-1}\Big(\frac{(g/2)+x}{y}\Big) + \tan^{-1}\Big(\frac{(g/2)-x}{y}\Big)\Big) \quad (1)$$

$$H_y(x,y) = \frac{1}{2\pi} H_0 \ln\Big(\frac{((g/2)-x)^2+y^2}{((g/2)+x)^2+y^2}\Big) \quad (2)$$

where g is the head gap, and H_0 is the deep gap field, given by:

$$H_0 = \frac{NEI}{g} \quad (3)$$

where N is the number of turns coils of wire around the head, and E is the head efficiency which can be calculated by:

$$E = \frac{1}{1 + \frac{lA_g}{\mu_r g}\int_{core} \frac{d\vec{l}}{A(l)}} \quad (4)$$

where A_g is the gap area, μ_r is the core permeability relative to free space (μ_0), and $A(l)$ is the cross-sectional area of the core as a function of length.

1.2. Tape Magnetisation

The magnetic field being recorded to tape can be described using a hysteresis loop, as follows [3]:

$$\vec{M}(x,y) = F_{Loop}(\vec{H}(x,y)) \quad (5)$$

where F_{Loop} is a generalized hysteresis function.

Using the Jiles-Atherton magnetisation model, the following differential equation describes magnetisation (M) as a function of magnetic field (H) [4]:

$$\frac{dM}{dH} = \frac{(1-c)\delta_M (M_{an}-M)}{(1-c)\delta k - \alpha(M_{an}-M)} + c\frac{dM_{an}}{dH} \quad (6)$$

where c is the ratio of normal and anhysteric initial susceptibilities, k is a measure of the width of the hysteresis loop, α is a mean field parameter, representing inter-domain coupling, and δ and δ_M are given by:

$$\delta = \begin{cases} 1 & \text{if H is increasing} \\ -1 & \text{if H is decreasing} \end{cases} \quad (7)$$

$$\delta_M = \begin{cases} 1 & \text{if } \delta \text{ and } M_{an}-M \text{ have the same sign} \\ 0 & \text{otherwise} \end{cases} \quad (8)$$

M_{an} is the anisotropic magnetisation given by:

$$M_{an} = M_s L\Big(\frac{H+\alpha M}{a}\Big) \quad (9)$$

where M_s is the magnetisation saturation, a characterizes the shape of the anhysteric magnetisation and L is the Langevin function:

$$L(x) = \coth(x) - \frac{1}{x} \quad (10)$$

1.3. Play Head

1.3.1. Ideal Playback Voltage

The ideal playback voltage as a function of tape magnetisation is given by [3]:

$$V(x) = NWEv\mu_0 \int_{-\infty}^{\infty} dx' \int_{-\delta/2}^{\delta/2} dy' \vec{h}(x'+x, y') \cdot \frac{\vec{M}(x',y')}{dx} \quad (11)$$

where N is the number of turns of wire, W is the width of the playhead, E is the playhead efficiency, v is the tape speed, and μ_0 is the permeability of free space. Note that $V(x) = V(vt)$ for constant v. $\vec{h}(x, y)$ is defined as:

$$\vec{h}(x, y) \equiv \frac{\vec{H}(x, y)}{NIE} \tag{12}$$

where $\vec{H}(x, y)$ can be calculated by eqs. (1) and (2).

1.3.2. *Loss Effects*

There are several frequency-dependent loss effects associated with playback, described as follows [1]:

$$V(t) = V_0(t)[e^{-kd}]\Big[\frac{1 - e^{-k\delta}}{k\delta}\Big]\Big[\frac{\sin(kg/2)}{kg/2}\Big] \tag{13}$$

for sinusoidal input $V_0(t)$, where k is the wave number, d is the distance between the tape and the playhead, g is the gap width of the play head, and δ is the thickness of the tape. The wave number is given by:

$$k = \frac{2\pi f}{v} \tag{14}$$

where f is the frequency and v is the tape speed.

2. DIGITIZING THE SYSTEM

2.1. Record Head

For simplicity, let us assume,

$$\vec{H}(x, y, t) = \vec{H}(0, 0, t) \tag{15}$$

In this case $H_y \equiv 0$, and $H_x \equiv H_0$. Thus,

$$H(t) = \frac{NEI(t)}{g} \tag{16}$$

or,

$$\hat{H}(n) = \frac{NE\hat{I}(n)}{g} \tag{17}$$

2.2. Hysteresis

Beginning from eq. (6), we can find the derivative of M w.r.t. time, as in [4]:

$$\frac{dM}{dt} = \frac{\frac{(1-c)\delta_M(M_s L(Q)-M)}{(1-c)\delta k-\alpha(M_s L(Q)-M)}\frac{dH}{dt} + c\frac{M_s}{a}\frac{dH}{dt}L'(Q)}{1 - c\alpha\frac{M_s}{a}L'(Q)} \tag{18}$$

where $Q = \frac{H+\alpha M}{a}$, and

$$L'(x) = \frac{1}{x^2} - \coth^2(x) + 1 \tag{19}$$

Note that eq. (18) can also be written in the general form for non-linear Ordinary Differential Equations:

$$\frac{dM}{dt} = f(t, M, \vec{u}) \tag{20}$$

where $\vec{u} = \begin{bmatrix} H \\ \dot{H} \end{bmatrix}$.

Using the trapezoidal rule for derivative approximation, we find:

$$\dot{\hat{H}}(n) = 2\frac{\hat{H}(n) - \hat{H}(n-1)}{T} - \dot{\hat{H}}(n-1) \tag{21}$$

We can use the Runge-Kutta 4th-order method [5] to find an explicit solution for $\hat{M}(n)$:

$$\begin{aligned}
k_1 &= Tf\Big(n-1, \hat{M}(n-1), \hat{\vec{u}}(n-1)\Big) \\
k_2 &= Tf\Big(n-\frac{1}{2}, \hat{M}(n-1) + \frac{k_1}{2}, \hat{\vec{u}}\Big(n-\frac{1}{2}\Big)\Big) \\
k_3 &= Tf\Big(n-\frac{1}{2}, \hat{M}(n-1) + \frac{k_2}{2}, \hat{\vec{u}}\Big(n-\frac{1}{2}\Big)\Big) \\
k_4 &= Tf\Big(n, \hat{M}(n-1) + k_3, \hat{\vec{u}}(n)\Big) \\
\hat{M}(n) &= \hat{M}(n-1) + \frac{k_1}{6} + \frac{k_2}{3} + \frac{k_3}{3} + \frac{k_4}{6}
\end{aligned} \tag{22}$$

We use linear interpolation to find the half-sample values used to calculate k_2 and k_3.

2.2.1. *Numerical Considerations*

To account for rounding errors in the Langevin function for values close to zero, we use the following approximation about zero, as in [4]:

$$L(x) = \begin{cases} \coth(x) - \frac{1}{x} & \text{for } |x| > 10^{-4} \\ \frac{x}{3} & \text{otherwise} \end{cases} \tag{23}$$

$$L'(x) = \begin{cases} \frac{1}{x^2} - \coth^2(x) + 1 & \text{for } |x| > 10^{-4} \\ \frac{1}{3} & \text{otherwise} \end{cases} \tag{24}$$

Additionally, $\tanh(x)$, and by extension $\coth(x)$ is a rather computationally expensive operation. With this in mind, for real-time implementation, we approximate $\coth(x)$ as the reciprocal of a Gaussian continued fraction for $\tanh(x)$ [6], namely

$$\tanh(x) = \cfrac{x}{1 + \cfrac{x^2}{3 + \cfrac{x^2}{5 + \cfrac{x^2}{7}}}} \tag{25}$$

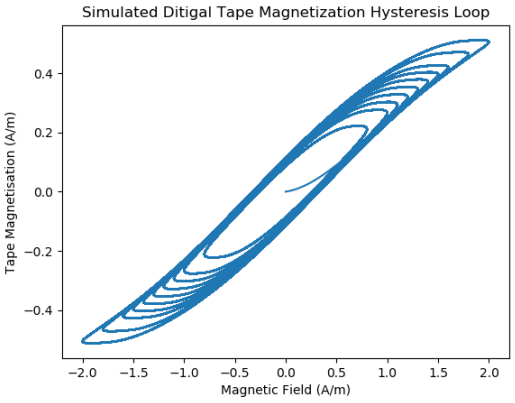

Figure 1: *Digitized Hysteresis Loop Simulation*

2.2.2. Simulation

The digitized hysteresis loop was implemented and tested offline in `Python`, using the constants M_s, a, α, k, and c from [7]. For a sinusoidal input signal with frequency 2kHz, and varying amplitude from 800 - 2000 Amperes per meter, fig. 1 shows the Magnetisation output.

2.3. Play Head

By combining eq. (11) with eqs. (12) and (16), we get:

$$V(t) = NWEv\mu_0 gM(t) \tag{26}$$

or,

$$\hat{V}(n) = NWEv\mu_0 g\hat{M}(n) \tag{27}$$

2.3.1. Loss Effects

In the real-time system, we model the playhead loss effects with an FIR filter, derived by taking the inverse DFT of the loss effects described in eq. (13). It is worth noting that as in eq. (14), the loss effects, and therefore the FIR filter are dependent on the tape speed.

The loss effects filter was implemented and tested offline in `Python` with tape-head spacing of 20 microns, head gap width of 5 microns, tape thickness of 35 microns, and tape speed of 15 ips. The following plot shows the results of the simulation, with a filter order of 100.

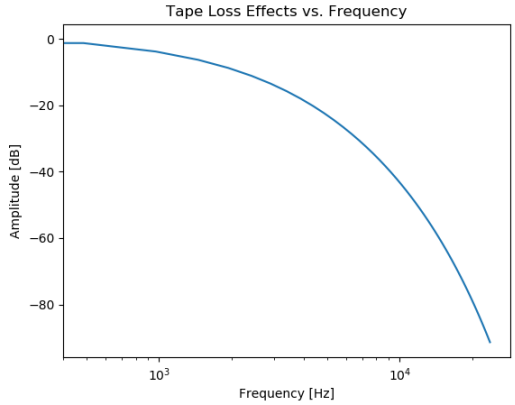

Figure 2: *Frequency Response of Playhead Loss Effects*

3. TAPE AND TAPE MACHINE PARAMETERS

In the following sections, we describe the implementation of a real-time model of a Sony TC-260 tape machine, while attempting to preserve generality so that the process can be repeated for any other similar reel-to-reel tape machine.

3.1. Tape Parameters

A typical reel-to-reel tape such as the Sony TC-260 uses Ferric Oxide ($\gamma F_2 O_3$) magnetic tape. The following properties of the tape are necessary for the tape hysteresis process eq. (18):

- Magnetic Saturation (M_s): For Ferric Oxide tape the magnetic saturation is $3.5e5$ (A/m) [8]
- Hysteresis Loop Width (k): For soft materials, k can be approximated as the coercivity, H_c [9]. For Ferric Oxide, H_c is approximately 27 kA/m [8].
- Anhysteric magnetisataion (a): Knowing the coercivity and remnance magnetism of Ferric Oxide [8], we can calculate a = 22 kA/m by the method described in [9]
- Ratio of normal and hysteris initial susceptibilities (c): From [9], c = 1.7e-1.
- Mean field parameter (α): From [9], α = 1.6e-3

3.2. Tape Machine Parameters

3.2.1. Record Head

To determine the magnetic field output of the record head using eq. (17), the following parameters are necessary:

- Input Current ($\hat{I}(n)$): For the Sony TC-260 the input current to the record head is approximately 0.1 mA peak-to-peak [10].
- Gap Width (g): The gap width for recording heads can range from 2.5 to 12 microns [1].
- Turns of wire (N): The number of turns of wire is typically on the order of 100 [3].
- Head Efficiency (E): The head efficiency is typically on the order of 0.1 [3].

These values result in a peak-to-peak magnetic field of approximately 5e5 A/m.

3.2.2. Play Head

Similar to the record head, the following parameters are needed to calculate the output voltage using eqs. (13) and (27) (note that values are only included here if notably different from the record head):

- Gap Width (g): The play head gap width ranges from 1.5 to 6 microns[1].
- Head Width (W): For the Sony TC-260, the play head width is 0.125 inches (note that this is the same as the width of one track on the quarter-inch tape used by the machine) [10].
- Tape Speed (v): The Sony TC-260 can run at 3.75 inches per second (ips), or 7.5 ips [10]. Note that many tape machines can run at 15 or 32 ips [1].
- Tape Thickness (δ): Typical tape that would be used with the TC-260 is on the order of 35 microns thick [10].
- Spacing (d): The spacing between the tape and the play head is highly variable between tape machines. For a typical tape machine spacing can be as high as 20 microns [1].

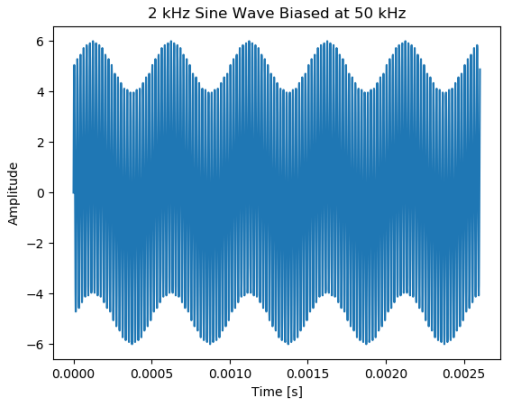

Figure 3: *Example of a biased signal*

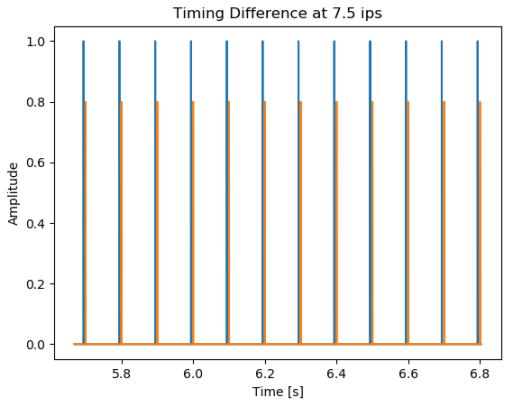

Figure 4: *Input pulse train superimposed with pulse train recorded from TC-260*

3.3. Tape Bias

A typical analog recorder adds a high-frequency "bias" current to the signal to avoid the "deadzone" effect when the input signal crosses zero, as well as to linearize the output. The input current to the record head can be given by [11]:

$$\hat{I}_{head}(n) = \hat{I}_{in}(n) + B\cos(2\pi f_{bias} nT) \tag{28}$$

Where the amplitude of the bias current B is usually about one order of magnitude larger than the input, and the bias frequency f_{bias} is well above the audible range. Figure 3 shows a unit-amplitude, 2 kHz sine wave biased by a 50 kHz sine wave with amplitude 5. To recover the correct output signal, tape machines use a lowpass filter, with a cutoff frequency well below the bias frequency, thought still above the audible range [1].

For the Sony TC-260, the bias frequency is 55 kHz, with a gain of 5 relative to the input signal. The lowpass filter used to recover the audible signal has a cutoff at 24 kHz, though note that due to the frequency response of the playhead loss effects, the effects of this filter may be essentially neglible to the real time system. [10]

3.4. Wow and Flutter

Each tape machine has characteristic timing imperfections known as “wow” and/or “flutter.” These imperfections are caused by minor changes in speed from the motors driving the tape reels, and can cause fluctuations in the pitch of the output signal. To characterize these timing imperfections, we use a method similar to [12]: We recorded a pulse train of 1000 pulses through a TC-260, then recorded the pulses back from the tape. Figure 4 shows a section of a superimposed plot of the original pulse train against the pulse train recorded from the tape machine. From this data, we were able to generate a periodic function that accurately models the timing imperfections of the TC-260. The process was performed at both 7.5 ips and 3.75 ips. In the real-time system, the timing imperfection model is used to inform a modulating delay line, to achieve the signature "wow" effect of an analog tape machine.

4. REAL-TIME IMPLEMENTATION

We implemented our physical model of the Sony TC-260 as a VST audio plugin using the JUCE framework. Figure 5 shows the signal flow of the system in detail. We allow the user to control parameters in real-time including the tape speed, bias gain, gap width, tape thickness, tape spacing, and flutter depth. C/C++ code for the real-time implementation is open-source and is available on GitHub [1].

4.1. Oversampling

If no oversampling is used, the system will be unstable for input signal at the Nyquist frequency, due to limitations of the trapezoid rule derivate approximation used in eq. (21). To avoid this instability, early versions of the real-time implementation used a lowpass filter with cutoff frequency just below Nyquist. However, due to aliasing caused by the nonlinearity of the tape hysteresis model, oversampling is necessary to mitigate aliasing artifacts [5]. Further, the system must be able to faithfully recreate not only the frequencies in the audible range but the bias frequency as well. Since the TC-260 uses a bias frequency of 55 kHz [10] and the minimum standard audio sampling rate is 44.1 kHz, a minimum oversampling factor of 3x is required. However, since the biased signal is then fed into the hystersis model, even more oversampling is required to avoid aliasing. With these considerations in mind, our system uses an oversampling factor of 16x.

4.2. Results

In subjective testing, our physical model sounds quite convincing, with warm, tape-like distortion, and realistic sounding flutter. The high-frequency loss and low-frequency “head bump” change correctly at different tape speeds, and are approximately within the frequency response specifications of the TC-260 service manual [10]. The distortion and frequency response characteristics of our model are subjectively very close when compared to the output of an actual TC-260, though not nearly close enough to “fool” the listener. Additionally, as the bias gain is lowered, the “deadzone”

[1] `https://github.com/jatinchowdhury18/AnalogTapeModel`

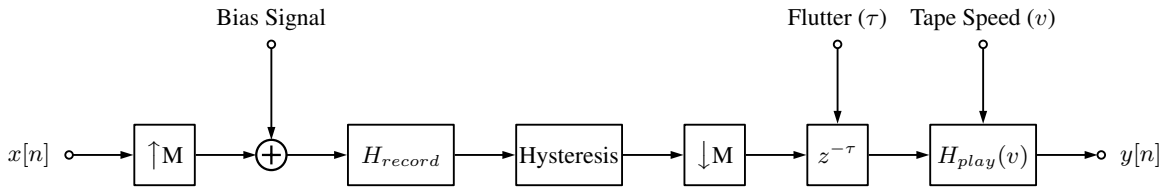

Figure 5: *Flowchart of realtime system: M is the oversampling factor, H_{record} is the transfer function of the record head, and H_{play} is the play head transfer function including loss effects, and a de-biasing filter.*

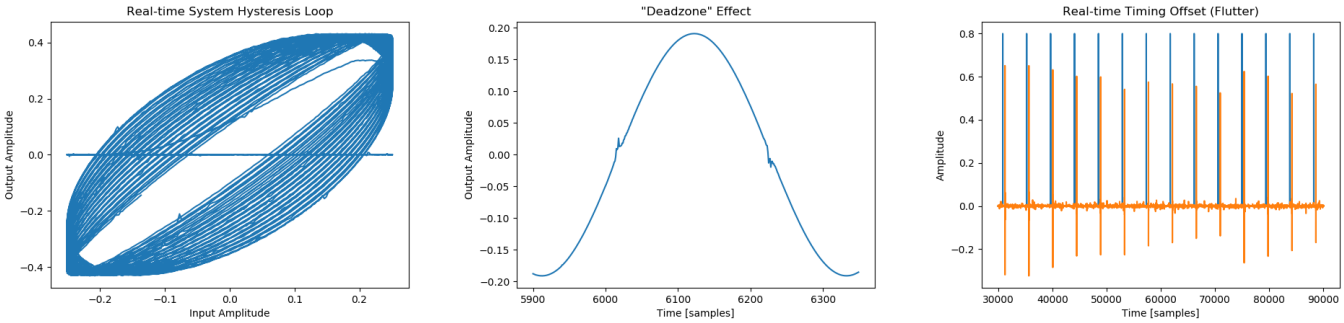

Figure 6: *Testing results for real-time system: input vs. output amplitude for variable frequency sine wave (left), sine wave output with no biasing (center), input vs. output pulse train comparison (right).*

effect appears exactly as expected [11]. The largest difference between the model and the physical machine is the subtle electrical and mechanical noises and dropouts present in the physical machine, presumably caused by the age and wear-and-tear of the machine, which we did not attempt to characterize in our model. Figure 6 shows the results of tests performed on the real-time system. In particular, note the successfully modelled hysteresis function (left), the "deadzone" effect (center), and the timing imperfections or flutter (right). Audio examples from the real-time system can be found online[2].

5. FUTURE IMPROVEMENTS

5.1. Spatial Magnetic Effects

The most obvious improvement to be made for the physical model is the inclusion of spatial effects of the tape. In particular, the approximations made in eq. (15), negate any effects caused by magnetisation along the longitudinal length of the tape, and into the depth of the tape. Including spatial effects would involve deriving digital analogues for eqs. (1), (2) and (11), and re-deriving eq. (22) to take an 2-dimensional magnetic field input at every timestep, rather than the zero-dimensional input it currently takes. This change would greatly increase the computational complexity of the system. At an oversampling rate of 16x, using just 100 spatial samples would be 1600x more computationally complex than the current system.

6. ACKNOWLEDGEMENTS

Many thanks to Julius Smith for guidance and support, and thanks to Irene Abosch for kindly donating her Sony TC-260.

[2] `https://ccrma.stanford.edu/~jatin/420/tape/`

7. REFERENCES

[1] Jay Kadis, *The Science of Sound Recording*, Focal Press, Waltham, MA, 1 edition, 2012.

[2] Brian Eno, *A Year with Swollen Appendices*, Faber and Faber, 1996.

[3] H. N. Bertram, *Theory of Magnetic Recording*, Apr. 1994.

[4] Martin Holters and Udo ZÃ¶lzer, "Circuit simulation with inductors and transformers based on the jiles-atherton model of magnetization," 09 2016.

[5] D.T. Yeh, *Digital Implementation of Musical Distortion Circuits by Analysis and Simulation*, Ph.D. thesis, Stanford Univeristy, 6 2009.

[6] Analytic Theory of Continued Fractions, *H. S. Wall*, Chelsea, New York, 1948.

[7] D. C. Jiles and D. L. Atherton, "Theory of ferromagnetic hysteresis," *Journal of Magnetism and Magnetic Materials*, vol. 61, pp. 48–60, Sept. 1986.

[8] D. Jiles, *Introduction to Magnetism and Magnetic Materials*, CRC Press, 2015.

[9] D. C. Jiles, J. B. Thoelke, and M. K. Devine, "Numerical determination of hysteresis parameters for the modeling of magnetic properties using the theory of ferromagnetic hysteresis," *IEEE Transactions on Magnetics*, vol. 28, pp. 27–35, Jan. 1992.

[10] Sony, "Sony tc-260 service manual," 1965.

[11] Marvin Camras, *Magnetic Recording Handbook*, Van Nostrand Reinhold Co., New York, NY, USA, 1987.

[12] Steinunn Arnardottir, Jonathan S. Abel, and Julius O. Smith III, "A digital model of the echoplex tape delay," in *Audio Engineering Society Convention 125*, Oct 2008.